Electronic Supplementary Material (ESI) for Dalton Transactions.

Supporting Information

High-efficiency counter electrodes for quantum dot-sensitized solar cells (QDSSCs): Designing Graphene-supported $CuCo_2O_4$ porous hollow microspheres with improved electron transport performance

Qiu Zhang, Tingting Zhang, Libo Wang, Fengyan Li *, Lin Xu *

Key Laboratory of Polyoxometalate and Reticular Material Chemistry of Ministry of Education, Department of Chemistry, Northeast Normal University, Changchun, Jilin 130024, P. R. China.

E-mail: lify525@nenu.edu.cn; linxu@nenu.edu.cn

1. Experimental section

1.1. Chemicals and materials

$Cu(NO_3)_2 \cdot 3H_2O$ (AR, ≥99.5%), $(NH_2)_2CO$ (AR, ≥99.0%), Terpineol ($C_{10}H_{18}O$, AR), NH_4Cl (AR, ≥99.0%), H_2NCSNH_2 (AR, ≥99.0%), $C_4H_6O_4Zn \cdot 2H_2O$ (AR, ≥99.0%), KCl (AR, ≥99.5%), Na_2SO_3 (AR, ≥97.0%), ammonium hydroxide, isopropanol, glycerol, absolute methanol and acetone were purchased from Sinopharm. $Na_2S \cdot 9H_2O$ (AR, ≥98.0%), $Co(NO_3)_2 \cdot 6H_2O$ (AR, ≥99%), polyvinylpyrrolidone (K30), Sulfur (S, 99.99%), Graphite powder (99.8%), Titanium oxide (TiO_2, Degussa, P25). $CdCl_2$ (AR, ≥99.0%), $Cd(OAc)_2$ (AR, 99.0%), $N(CH_2COONa)_3$ (AR, 98.0%), selenium powder (Se, 200 mesh, 99.9%) were purchased from Aladdin (Sigma-Aldrich).

1.2. Characterizations

X-ray powder diffraction test was conducted from 15 to 80° adopting Siemens D5005 diffractometer with Cu target Kα (λ = 1.5418 Å) rays as X-ray source. A field emission scanning electron microscope (SEM JEOL JSM 4800F) equipped with X-ray energy dispersion (EDX) analysis was used to study the surface morphology and element composition of the samples. X-ray photoelectron spectroscopy (XPS) was carried out applying an ESCALABMKII spectrometer and the X-ray source was achromatic Al-Ka (1486.6 eV). The electron transmission microscopy (TEM) and HRTEM images was received using the transmission electron microscope JEOL-2100F. The datas of nitrogen adsorption–desorption isotherms were collected from an ASAP 2020 (Micromeritics, USA). An IVIUM purchased from Tianjin Brillante Technology Limited with a filtered 500 W Xenon lamp is utilized to current–voltage (I–V) curves measurements under the condition of AM 1.5 100 mW/cm^2. Incident photon-to-current efficiency (IPCE) was received by BUNKOKEIKI CEP-2000. The EIS, Tafel, CV and open circuit voltage decay (OCVD) tests are all used CHI660D electrochemical workstation (Shanghai Chenhua, China). EIS test conditions: the frequency range is 10^{-1}-10^5 Hz; the amplitude is 0.01 V, which is performed under the condition of open-circuit voltage. All characterizations were conducted at ambient temperature and pressure.

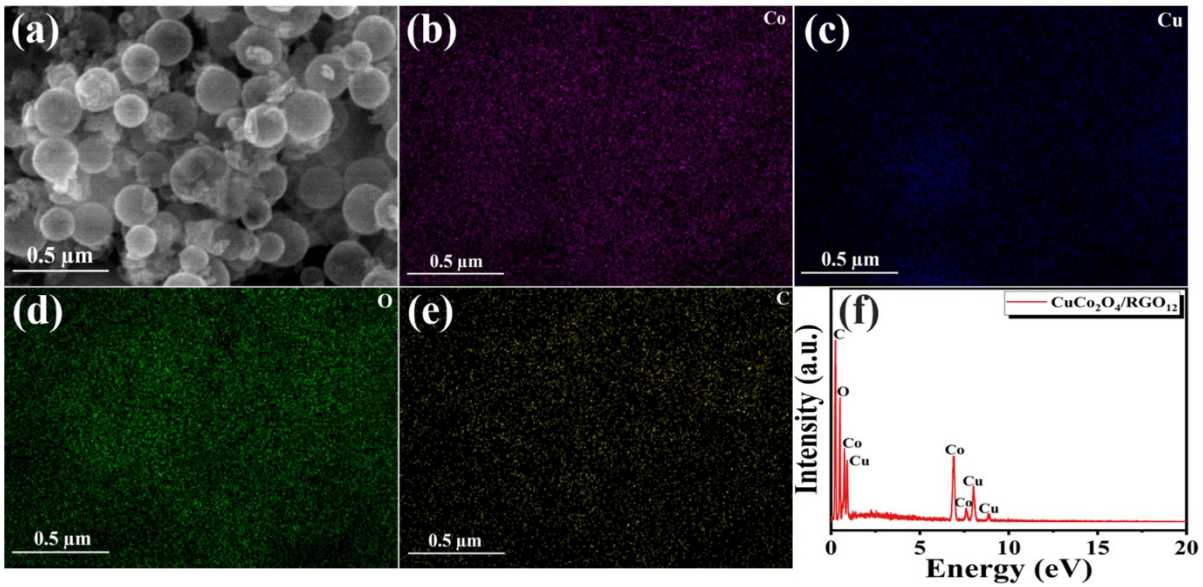

Fig. S1. (a–e) EDX elemental mappings of Co (b), Cu (c), O (d), C (e) and (f) EDX image in the $CuCo_2O_4/RGO_{12}$ composite.

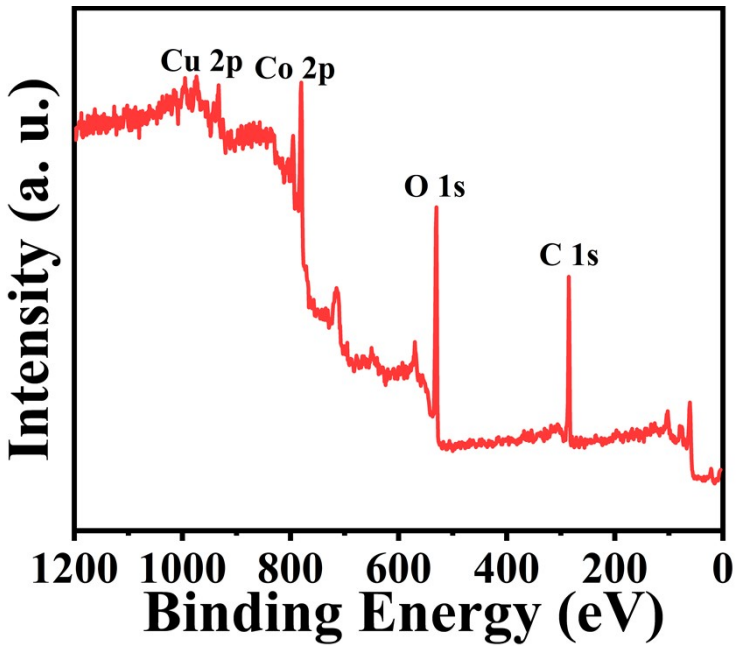

Fig. S2. XPS survey scan spectrum of $CuCo_2O_4/RGO_{12}$ composite.

Table S1 Comparison of QDSSCs performance with other reported counter electrodes.

Counter electrode	J_{sc} (mA/cm^2)	V_{oc} (V)	FF	PCE (%)	Ref.
$Cu_{1.18}S$-GOR	20.55	0.626	0.53	6.81	1
BCNT	17.40	0.520	0.52	4.55	2
$CoSe_2$-NC	19.65	0.540	0.48	5.06	3
g-C_3N_4/NiS	17.56	0.570	0.56	5.64	4
Cu_2S@SLG	3.74	0.500	0.63	3.93	5
$MnCo_2S_4$/CNTs	18.45	0.580	0.45	4.85	6
MoS_2/CNT	20.16	0.620	0.40	5.05	7
Ti/Cu_2S	16.31	0.570	0.44	4.11	8
alpha-MoO_3-C	1.29	0.48	0.31	1.29	9
$Cu_{2-x}Se/Cu_7S_4$	23.02	0.517	0.36	4.38	10
CB/Cu_xS	16.96	0.584	0.567	5.62	11
RGO-Cu_2S	15.85	0.556	0.44	3.85	12
Cu_2ZnSnS_4	13.40	0.730	0.67	6.19	13
Flower-like $CuCo_2O_4$@RGO	12.11	0.79	0.64	6.11	14
NiS-rGO	5.55	0.80	0.32	1.42	15
RGO/SnO_2/PANI	18.60	0.708	0.63	7.92	16
$CuCo_2O_4$	21.83	0.60	0.47	6.19	This work
$CuCo_2O_4$/RGO_{12}	22.83	0.61	0.51	7.04	This work

References

1 D. Ghosh, G. Halder, A. Sahasrabudhe and S. Bhattacharyya, Nanoscale, 2016, **8**, 10632.

2 W. Li, S. Zhang, Q. Chen and Q. Zhong, Catal. Sci. Technol., 2021, **11**, 2745-2752.

3 W. Li, M. Zheng, Z. Tian, G. Long, S. Zhang, Q. Chen and Q. Zhong, ECS J. Solid State Sci. Tecnnol., 2021, **10**, 045012.

4 W. Li, Q. Chen and Q. Zhong, J. Mater. Sci., 2020, **55**, 10712-10724.

5 E. Akman, Y. Altintas, M. Gulen, M. Yilmaz, E. Mutlugun and S. Sonmezoglu, Renew. Energ., 2020, **145***,* 2192-2200.

6 W. Li, L. He, J. Zhang, B. Li, Q. Chen and Q. Zhong, J. Phys. Chem. C, 2019, **123,** 21866-21873.

7 H. Yan, Z. Qi, Q. Chen and Q. Zhong, ECS J. Solid State Sci. Technol., 2019, **8**, P77-P82.

8 J. Chae, M. Oh, V. H. V. Quy, J. Kwon, J.-H. Kim, S.-H. Kang, H. Kim, E. Vijayakumar and K.-S. Ahn, Thin Solid Films, 2018, **660**, 46-53.

9 P. S. Tamboli, M. B. R. Prasad, V. S. Kadam, R. S. Vhatkar, Inamuddin; H. M. Pathan and S. S. Mahajan, Sol. Energy Mater. Sol. Cells, 2017, **161**, 96-101.

10 L. Ran and L. Yin, CrystEngComm, 2017, **19**, 5640-5652.

11 I. P. Liu, H. Teng and Y.-L. Lee, J. Mater. Chem. A, 2017, **5**, 23146-23157.

12 M. Ye, C. Chen, N. Zhang, X. Wen, W. Guo and C. Lin, Adv. Energy Mater., 2014, **4**, 1301564.

13 Y. Li, M. Yang, Y. Huang, X. Sun, K. Liu and J. Zhang, Solid State Sci., 2021, **113,** 106547.

14 K. Xiong, W. Nie, P. Yu, L. Zhu and X. Xiao, Mater. Lett., 2017, **204**, 69-72.

15 S. A. Salleh, M. Y. A. Rahman and T. H. T. Aziz, Inorg. Chem. Commun., 2022, **135**, 109086.

16 M. A. K. L. Dissanayake, J. M. K. W. Kumari, G. K. R. Senadeera and H. Anwar, Sol. Energy, 2021, **230**, 151-165.